ACS Energy LETTERS

http://pubs.acs.org/journal/aelccp

Bifunctional Surface Engineering on SnO_2 Reduces Energy Loss in Perovskite Solar Cells

Eui Hyuk Jung,[‡] Bin Chen,[‡] Koen Bertens, Maral Vafaie, Sam Teale, Andrew Proppe, Yi Hou, Tong Zhu, Chao Zheng, and Edward H. Sargent*

Cite This: *ACS Energy Lett.* 2020, 5, 2796−2801

Read Online

ACCESS | Metrics & More | Article Recommendations | Supporting Information

ABSTRACT: **Tin oxide (SnO_2) has recently emerged as a promising electron transport layer for perovskite solar cells (PSCs) in light of the material's optical and electronic properties and its low-temperature processing. However, SnO_2 films are prone to surface defect formation, which results in energy loss in PSCs. We report that surface treatment using ammonium fluoride (NH_4F) leads to reduced surface defects and that it also induces chemical doping of the SnO_2 substrate simultaneously. The effects of NH_4F treatment on SnO_2 properties are revealed by surface chemical analysis, computational studies, and energy level investigations, and PSCs with the treatment achieve photovoltaic performance of 23.2% in light of higher voltage than in relevant controls.**

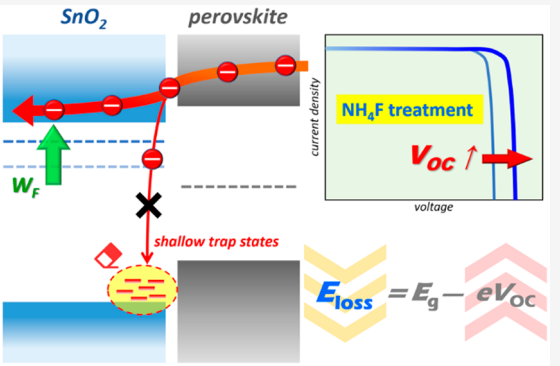

Metal oxide semiconductors have contributed to the development of perovskite solar cells (PSCs) by providing selective contacts.[1−3] In early research on PSCs, mesoporous titanium oxide (TiO_2) electron transport layers (ETLs) were used, but these required high-temperature processes over 450 °C.[4] Research has recently shifted to tin oxide (SnO_2)-based electron transport layers because of their higher electron mobility,[5] reduced optical losses because of higher transmittance, and smaller refractive index difference between transparent conductive oxides (TCOs) such as indium tin oxide (ITO) or fluorine-doped tin oxide (FTO) composed of SnO_x,[6,7] as well as low-temperature processing.[8] The record for the highest PSC photovoltaic performance is held by devices that use a SnO_2 ETL.[3]

Despite the excellence of SnO_2, the SnO_2 layer does have a drawback: metal oxides contain surface hydroxyl groups, and these generate trap states near the valence band.[9] It is important to reduce the defect sites on the SnO_2 surface because these cause nonradiative recombination at the SnO_2/perovskite interface. There is also room to improve the electron extraction from the perovskite by tuning the SnO_2 energy level via doping.[10,11]

Here we report a bifunctional surface treatment that uses ammonium fluoride (NH_4F) to reduce defect sites and adjust the Fermi level of SnO_2 thin films. This concept was inspired by the preparation of fluorine-doped SnO_2 (FTO) by reaction with tin(IV) tetrahydroxide ($Sn(OH)_4$) and NH_4F.[12] We theorized that an NH_4F surface treatment could eliminate hydroxyl groups from the SnO_2 surface and also dope it with fluorine ions (Figure 1a). In agreement with previous literature, we determined that two kinds of hydroxyl groups exist on metal oxide surface: terminal-hydroxyls (OH_T), which bind to one metal site with a basic characteristic, and bridge-hydroxyls (OH_B), which bind to two metal sites with an acidic characteristic.[13] We expected that an ammonium cation with weak acidity from NH_4F would react with the OH_T on the SnO_2 surface, forming ammonia gas and water vapor, and fluoride anions would substitute into the defect sites leading to tuning of the energy level.

We tested this idea by analyzing X-ray photoelectron spectroscopy (XPS) data for a pristine SnO_2 surface versus an NH_4F-treated SnO_2 surface (Figure 1b,c). The XPS spectra of O 1s for both samples (left column) show two distinct peaks for different oxygen species. A peak at 532.2 eV indicates the presence of a hydroxyl (−OH) group on the SnO_2 surface, and another peak at 530.3 eV originates from the saturated oxygen in SnO_2.[14] By comparing the XPS spectra of O 1s, one sees that the ratio of hydroxyl group peak to saturated oxide peak is reduced from I_{OH}/I_{O_2}= 1.85 (control) to 0.78 (NH_4F).

Received: July 20, 2020
Accepted: August 4, 2020
Published: August 4, 2020

https://dx.doi.org/10.1021/acsenergylett.0c01566
ACS Energy Lett. 2020, 5, 2796−2801

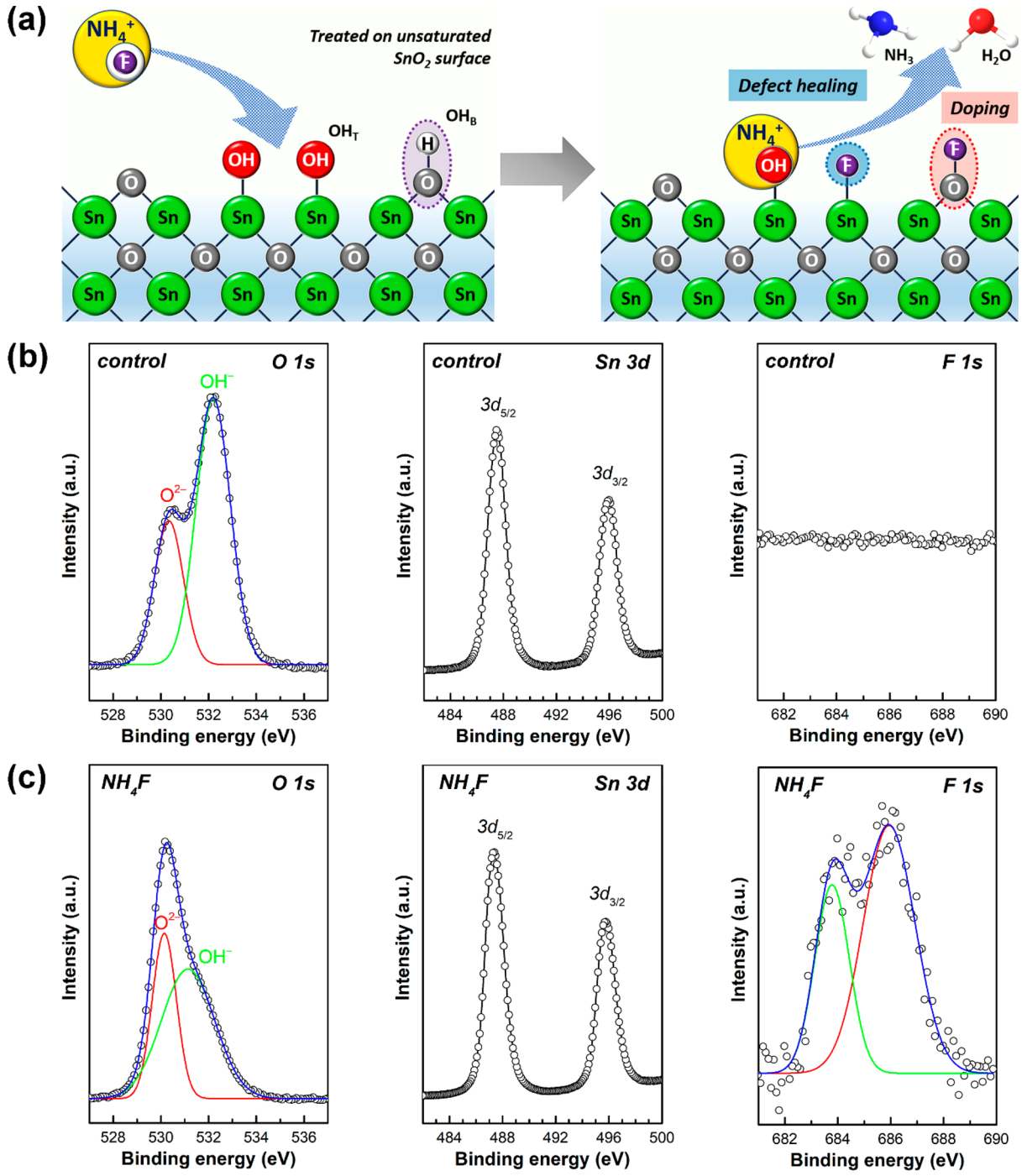

Figure 1. (a) Schematic illustration of NH_4F treatment on SnO_2 surface. XPS spectra of O 1s, Sn 3d, and F 1s for (b) pristine SnO_2 (control) and (c) NH_4F-treated SnO_2 (NH_4F). All SnO_2 substrates were prepared via a chemical bath deposition method.

In the Sn 3d XPS spectra of each sample (middle column), the peaks shows an 8.4 eV difference, consistent with the tetravalent oxidation state of tin in SnO_2.[15] The two peaks for the NH_4F-treated SnO_2 are downshifted 0.2 eV toward a lower binding energy compared to pristine SnO_2. In terms of fluorine (right column), the XPS spectrum of the NH_4F-treated SnO_2 shows doublet peaks, while that for pristine SnO_2 exhibits no signal. The fluorine signal indicates that NH_4F treatment induces fluorination on SnO_2 accompanying chemical doping. From XPS results of Sn 3d and F 1s for both samples, we conclude that the NH_4F treatment leads to the incorporation of fluorine on the SnO_2 surface.

We employed density functional theory (DFT) to explore the effects of the NH_4F treatment on the electronic properties of the SnO_2 surface. We chose the stoichiometric (110) surface for the study as it is the most thermodynamically stable configuration.[8,16] This is in line with XPS spectra, which indicate that Sn is in the 4^+ state (Figure 1b), rather than the reduced 2^+ state which is typically found in a non-stoichiometric, oxygen-deficient surface.[17] There are two main active sites on the surface; one is the bridge oxygen, and the other is the 5-fold-coordinated Sn (Figure 2a). The surface chemistry is determined by these dangling bonds, because they readily interact with water to form hydroxyl

https://dx.doi.org/10.1021/acsenergylett.0c01566
ACS Energy Lett. 2020, 5, 2796−2801

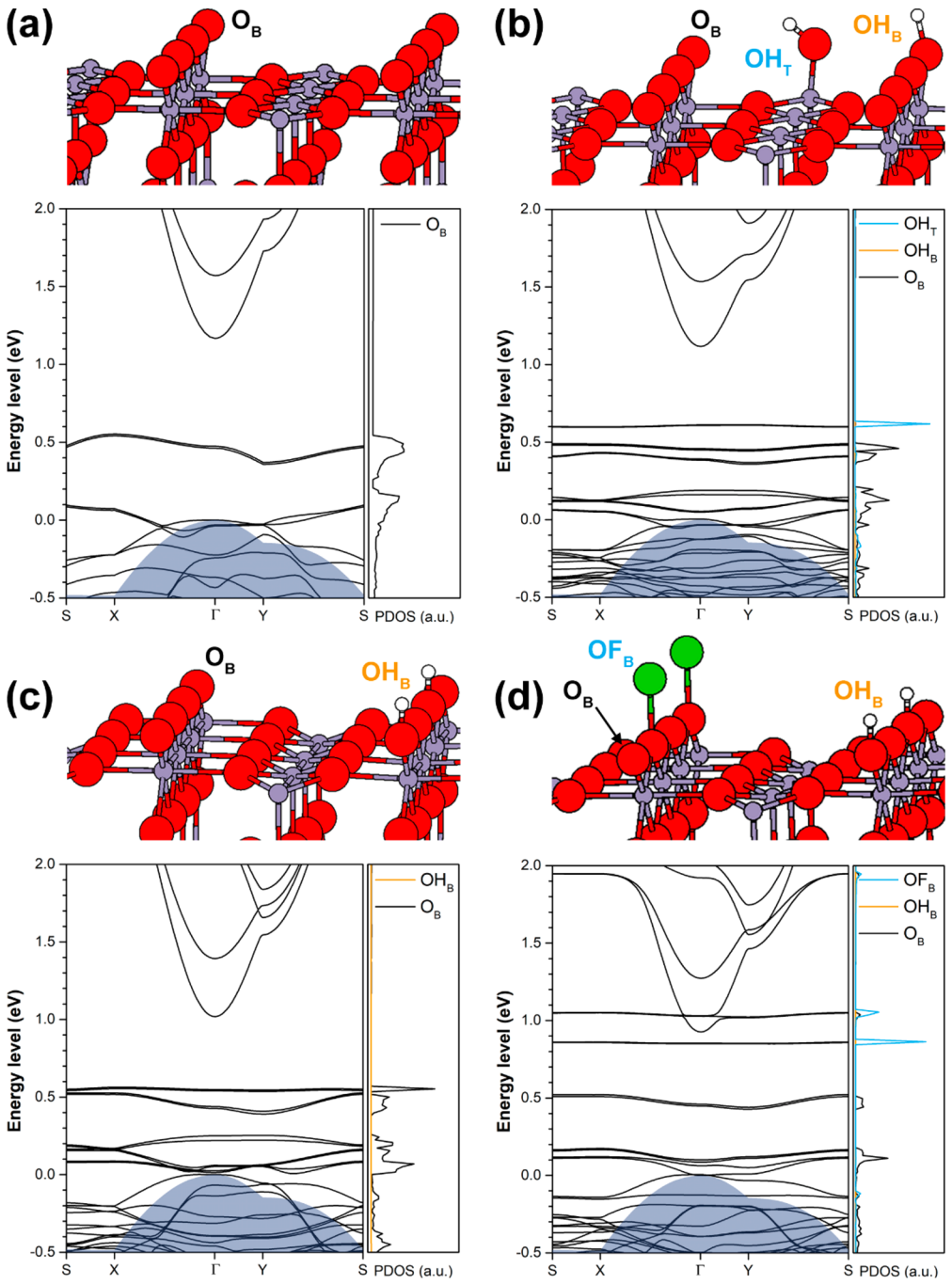

Figure 2. Band structure and partial density of states (PDOS) of various (110) SnO_2 surfaces: (a) stoichiometric surface where O_B indicates bridge oxygen; (b) hydroxylated surface; (c) OH_B-only surface after OH_T neutralizes with ammonium cation (NH_4^+); (d) OH_B-only surface with fluorine doping atop bridge oxygen site (OF_B). Gray shaded area represents the valence band maximum of bulk SnO_2.

groups (Figure S1a).[13,17] The under-coordinated metal atoms serve as Lewis acid attracting water molecules, and these dissociate and form two types of hydroxyl groups (Figure 2b) by transferring a proton to the nearby oxide ion.[13] The XPS spectrum confirms the presence of an −OH peak and the absence of an H_2O peak (Figure 1b).

Figure 2a shows the band structure and the partial density of states (PDOS) of the stoichiometric (110) SnO_2 surface. The shaded area is the contribution from the bulk SnO_2 valence band maximum (VBM), and it serves as an energy reference across the different surface configurations. We note that the OH_T in the hydroxylated surface introduces deep energy states in the bandgap (Figure 2b), which are traps that produce nonradiative recombination and result in energy loss.

We consider the following four cases when the hydroxylated surface is treated using NH_4F. The first and the most prominent reaction is between the ammonium cation and the OH_T group, because OH_T is basic and tends to dissociate as an −OH anion.[13] XPS shows that the concentration of hydroxyl groups is reduced by 58% after NH_4F treatment (Figure 1c). It is reasonable that most of the removed hydroxyl groups are OH_T because of its basic nature and readiness to react with NH_4^+, while doubly bonded OH_B is harder to remove. DFT predicts that the removal of terminal hydroxyl

https://dx.doi.org/10.1021/acsenergylett.0c01566
ACS Energy Lett. 2020, 5, 2796−2801

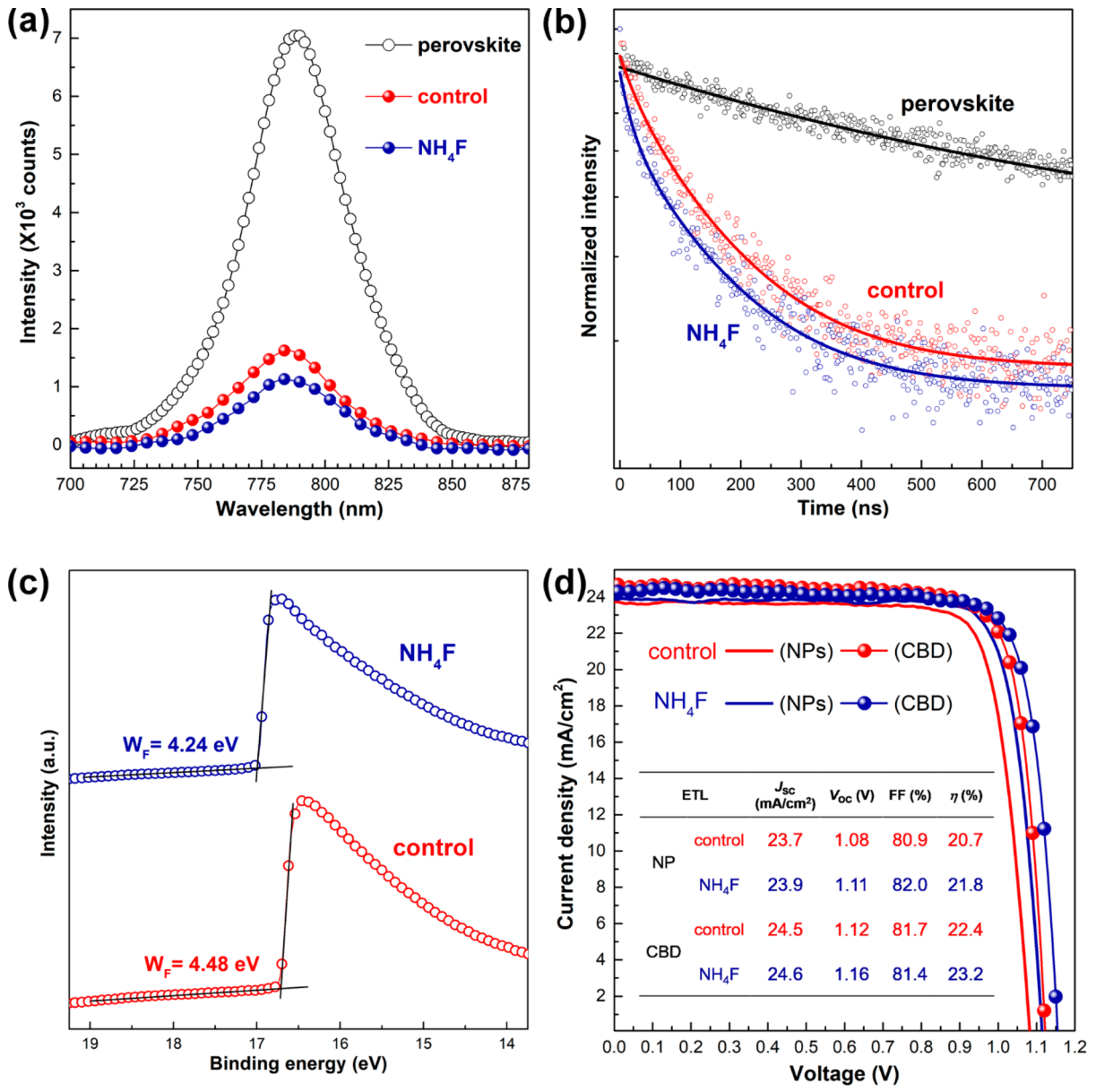

Figure 3. (a) Steady-state photoluminescence spectrum and (b) time-resolved photoluminescence decay curves of perovskite films on glass, pristine SnO_2 (control), and NH_4F-treated SnO_2 (NH_4F) substrates. (c) UPS spectra of pristine SnO_2 (control) and NH_4F-treated SnO_2 (NH_4F). (d) $J-V$ curves of perovskite solar cells based on pristine (red curves) and NH_4F-treated (blue curves) SnO_2 electron transport layers. NPs and CBD indicate preparation methods for the SnO_2 layers (NP, spin-coating using SnO_2 nanoparticle dispersion; CBD, chemical bath deposition).

groups eliminates trap states and thus can potentially improve the open-circuit voltage (V_{OC}) of a PSC (Figure 2c). In a second probable reaction with a terminal hydroxyl group, it is replaced with a fluorine atom through anion exchange, forming a terminal fluorine (F_T). The XPS spectrum of treated SnO_2 shows both a substitutional fluorine peak and another fluorine peak with a higher electron binding energy (Figure 1c). It is likely to be F_T, as the singly bonded fluorine accepts a reduced proportion of the electron density from Sn compared to the doubly bonded substitutional fluorine. Therefore, F_T creates a more positive electrostatic potential to bind more strongly with the electron. DFT also predicts the removal of OH_T trap states upon fluorine exchange (Figure S1b). The third scenario is the substitution of the bridge oxygen by fluorine, which is predicted to have a minimal effect on the band structure as it does not introduce trap states (Figure S1c). In the last case, where the fluorine bonds to a bridge oxygen, the electronic structure of the SnO_2 is significantly affected in terms of *n*-type doping (Figure 2d). Fluorine directly contributes to the shallow states below the conduction band minimum (CBM).

We investigated charge-transfer properties to study the effects of NH_4F treatment at the perovskite/SnO_2 interface. We did so by conducting a suite of photoluminescence (PL) spectroscopy measurements. The steady-state PL spectra (Figure 3a) show a higher quenching efficiency of 84% for NH_4F-treated samples, while pristine SnO_2 has a quenching efficiency of 77%, indicating that NH_4F treatment modifies the SnO_2 surface to favor electron extraction from the perovskite film. Figure 3b shows the time-resolved PL decay curves for the corresponding samples. The curves were fit using a

https://dx.doi.org/10.1021/acsenergylett.0c01566
ACS Energy Lett. 2020, 5, 2796−2801

biexponential decay function, yielding a fast decay (τ_1) and a slow decay (τ_2) component. The commonly accepted photophysical interpretation for perovskite/charge selective layer interfaces is that τ_1 originates from the quenching of charge carries by the charge selective layers, and τ_2 is attributed to radiative recombination of free charge carriers in perovskite bulk.[18,19] The lifetimes of the NH_4F-treated sample were calculated as having τ_1 of 20 ns and τ_2 of 143 ns, while the control sample showed a larger τ_1 of 30 ns and a comparable τ_2 of 146 ns, indicating that the NH_4F treatment leads to dynamically faster electron extraction.

Ultraviolet photoelectron spectroscopy (UPS) measurements were performed to estimate the work function (W_F) shift after NH_4F treatment on SnO_2. Figure 3c shows that the photoemission cutoff for NH_4F-treated SnO_2 is 16.98 eV, corresponding to a W_F of 4.24 eV, while pristine SnO_2 has a W_F of 4.48 eV. The NH_4F treatment upshifts the Fermi energy level of SnO_2 by 0.24 eV, a finding we attribute to fluorine doping of SnO_2.[20] The W_F shift via NH_4F treatment is consistent with the DFT calculation results that fluorine substitution on the SnO_2 surface generates doping energy levels near the conduction band minimum of SnO_2. The reduced W_F from the NH_4F treatment indicates that the Fermi energy level of SnO_2 shifts further from that of the perovskite, enlarging the built-in-potential for the photovoltaic device. We evaluated current−voltage plots of ITO/SnO_2/perovskite/Au to understand the effect of NH_4F treatment on resistance on SnO_2 (Figure S2). Resistances obtained from the slope of the plots indicate NH_4F treatment barely influences the charge transport properties of SnO_2.

To explore the impact of NH_4F-treated SnO_2 on photovoltaic performance, we fabricated devices on a TCO (ITO or FTO)/SnO_2/$(FAPbI_3)_{0.95}(MAPbBr_3)_{0.05}$/spiro-OMeTAD/Au configuration, a planar n-i-p structure, and characterized performance (Figure 3d). We employed two kinds of SnO_2 substrates: spin-coating of a commercial SnO_2 nanoparticle dispersion on an ITO substrate and vertically dipping an FTO substrate in tin chloride solution, known as chemical bath deposition (CBD).[21] When we used the nanoparticle (NP)-based ETL, devices with NH_4F-treated SnO_2 showed an improved power conversion efficiency (PCE) compared to that of control devices. Regarding devices made using CBD, devices with NH_4F-treated SnO_2 also achieved an improved PCE of 23.2% with a short-circuit current density (J_{SC}) of 24.6 mA/cm^2, a V_{OC} of 1.16 V, and a fill factor (FF) of 81.4%, while the control device showed 22.4% with a V_{OC} of 1.12 V. These results were evaluated for statistical significance by comparing the PCE and V_{OC} data from the 12 devices (Figure S3). As comparing to NP-based and CBD-based devices, CBD-based devices showed higher performance regardless of NH_4F treatment. It might result from the roughness difference between both as discussed in previous literature.[22] SnO_2 prepared by CBD on FTO substrate may have higher contact with perovskite film to allow more efficient electron extraction compared to SnO_2 prepared by spinning NP on the ITO substrate. The V_{OC} improvement upon NH_4F treatment is attributed to healing of defects and fluorine doping on the SnO_2 surface, because energy loss at the perovskite/charge selective layer interface is caused by surface defects and energy level alignment.[23] We measured current density−voltage curves along both bias scanning directions and also stabilized PCEs at the maximum power point. CBD-based devices treated with NH_4F showed negligible current hysteresis and enhanced stabilized PCE (Figures S4 and S5). We offer that NH_4F treatment on SnO_2 in PSCs leads to the enhanced V_{OC} by reducing energy loss at the SnO_2/perovskite interface.

The bifunctional surface engineering strategy on SnO_2 using NH_4F heals surface defects and favorably tunes the Fermi energy level of SnO_2, as seen in XPS, UPS, and DFT calculations. PL measurements show this strategy renders SnO_2 substrates more efficient in electron transfer from the perovskite film. The surface modification leads to reduced energy losses in PSCs, resulting in improved efficiency.

■ ASSOCIATED CONTENT

Supporting Information

The Supporting Information is available free of charge at https://pubs.acs.org/doi/10.1021/acsenergylett.0c01566.

Materials, device fabrication and characterization, and Figures S1−S5 (PDF)

■ AUTHOR INFORMATION

Corresponding Author

Edward H. Sargent − *The Edward S. Rogers Department of Electrical and Computer Engineering, University of Toronto, Toronto, Ontario, Canada M5S 3G4;* orcid.org/0000-0003-0396-6495; Email: ted.sargent@utoronto.ca

Authors

Eui Hyuk Jung − *The Edward S. Rogers Department of Electrical and Computer Engineering, University of Toronto, Toronto, Ontario, Canada M5S 3G4;* orcid.org/0000-0002-2833-522X

Bin Chen − *The Edward S. Rogers Department of Electrical and Computer Engineering, University of Toronto, Toronto, Ontario, Canada M5S 3G4*

Koen Bertens − *The Edward S. Rogers Department of Electrical and Computer Engineering, University of Toronto, Toronto, Ontario, Canada M5S 3G4*

Maral Vafaie − *The Edward S. Rogers Department of Electrical and Computer Engineering, University of Toronto, Toronto, Ontario, Canada M5S 3G4;* orcid.org/0000-0001-9119-6499

Sam Teale − *The Edward S. Rogers Department of Electrical and Computer Engineering, University of Toronto, Toronto, Ontario, Canada M5S 3G4;* orcid.org/0000-0001-9638-3453

Andrew Proppe − *The Edward S. Rogers Department of Electrical and Computer Engineering, University of Toronto, Toronto, Ontario, Canada M5S 3G4;* orcid.org/0000-0003-3860-9949

Yi Hou − *The Edward S. Rogers Department of Electrical and Computer Engineering, University of Toronto, Toronto, Ontario, Canada M5S 3G4;* orcid.org/0000-0002-1532-816X

Tong Zhu − *The Edward S. Rogers Department of Electrical and Computer Engineering, University of Toronto, Toronto, Ontario, Canada M5S 3G4*

Chao Zheng − *The Edward S. Rogers Department of Electrical and Computer Engineering, University of Toronto, Toronto, Ontario, Canada M5S 3G4*

Complete contact information is available at: https://pubs.acs.org/10.1021/acsenergylett.0c01566

https://dx.doi.org/10.1021/acsenergylett.0c01566
ACS Energy Lett. 2020, 5, 2796−2801

Author Contributions

‡E.H.J. and B.C. contributed equally to this work.

Notes

The authors declare no competing financial interest.

■ ACKNOWLEDGMENTS

This research was made possible by Ontario Research Fund-Research Excellence program (ORF7 Ministry of Research and Innovation, Ontario Research Fund-Research Excellence Round 7) and by the Natural Sciences and Engineering Research Council (NSERC) of Canada. This work was in part supported by the U.S. Department of the Navy, Office of Naval Research (N00014-17-1-2524). This research was also supported by the National Research Foundation of Korea (NRF) funded by NRF-2019R1A6A3A03032792.

■ REFERENCES

(1) Jena, A. K.; Kulkarni, A.; Miyasaka, T. Halide Perovskite Photovoltaics: Background, Status, and Future Prospects. *Chem. Rev.* **2019**, *119* (5), 3036−3103.

(2) Jung, E. H.; Jeon, N. J.; Park, E. Y.; Moon, C. S.; Shin, T. J.; Yang, T.-Y.; Noh, J. H.; Seo, J. Efficient, stable and scalable perovskite solar cells using poly(3-hexylthiophene). *Nature* **2019**, *567* (7749), 511−515.

(3) Jiang, Q.; Zhao, Y.; Zhang, X.; Yang, X.; Chen, Y.; Chu, Z.; Ye, Q.; Li, X.; Yin, Z.; You, J. Surface passivation of perovskite film for efficient solar cells. *Nat. Photonics* **2019**, *13* (7), 460−466.

(4) Kojima, A.; Teshima, K.; Shirai, Y.; Miyasaka, T. Organometal Halide Perovskites as Visible-Light Sensitizers for Photovoltaic Cells. *J. Am. Chem. Soc.* **2009**, *131* (17), 6050−6051.

(5) Park, M.; Kim, J.-Y.; Son, H. J.; Lee, C.-H.; Jang, S. S.; Ko, M. J. Low-temperature solution-processed Li-doped SnO_2 as an effective electron transporting layer for high-performance flexible and wearable perovskite solar cells. *Nano Energy* **2016**, *26*, 208−215.

(6) Ke, W.; Fang, G.; Liu, Q.; Xiong, L.; Qin, P.; Tao, H.; Wang, J.; Lei, H.; Li, B.; Wan, J.; Yang, G.; Yan, Y. Low-Temperature Solution-Processed Tin Oxide as an Alternative Electron Transporting Layer for Efficient Perovskite Solar Cells. *J. Am. Chem. Soc.* **2015**, *137* (21), 6730−6733.

(7) Liu, D.; Wang, Y.; Xu, H.; Zheng, H.; Zhang, T.; Zhang, P.; Wang, F.; Wu, J.; Wang, Z.; Chen, Z.; Li, S. SnO_2-Based Perovskite Solar Cells: Configuration Design and Performance Improvement. *Solar RRL* **2019**, *3* (2), 1800292.

(8) Jiang, Q.; Zhang, L.; Wang, H.; Yang, X.; Meng, J.; Liu, H.; Yin, Z.; Wu, J.; Zhang, X.; You, J. Enhanced electron extraction using SnO_2 for high-efficiency planar-structure $HC(NH_2)_2PbI_3$-based perovskite solar cells. *Nat. Energy* **2017**, *2* (1), 16177.

(9) Jia, J.; Qian, C.; Dong, Y.; Li, Y. F.; Wang, H.; Ghoussoub, M.; Butler, K. T.; Walsh, A.; Ozin, G. A. Heterogeneous catalytic hydrogenation of CO_2 by metal oxides: defect engineering − perfecting imperfection. *Chem. Soc. Rev.* **2017**, *46* (15), 4631−4644.

(10) Lee, J. H.; Shin, D.; Rhee, R.; Yun, S.; Yeom, K. M.; Chun, D. H.; Lee, S.; Kim, D.; Yi, Y.; Noh, J. H.; Park, J. H. Band Alignment Engineering between Planar SnO_2 and Halide Perovskites via Two-Step Annealing. *J. Phys. Chem. Lett.* **2019**, *10* (21), 6545−6550.

(11) Zhou, N.; Cheng, Q.; Li, L.; Zhou, H. Doping effects in SnO_2 transport material for high performance planar perovskite solar cells. *J. Phys. D: Appl. Phys.* **2018**, *51* (39), 394001.

(12) Wang, H.; Fu, F.; Zhang, F.; Wang, H.-E.; Kershaw, S. V.; Xu, J.; Sun, S.-G.; Rogach, A. L. Hydrothermal synthesis of hierarchical SnO_2 microspheres for gas sensing and lithium-ion batteries applications: Fluoride-mediated formation of solid and hollow structures. *J. Mater. Chem.* **2012**, *22* (5), 2140−2148.

(13) Boehm, H. P. Acidic and basic properties of hydroxylated metal oxide surfaces. *Discuss. Faraday Soc.* **1971**, *52* (0), 264−275.

(14) Gaggiotti, G.; Galdikas, A.; Kačiulis, S.; Mattogno, G.; Šetkus, A. Surface chemistry of tin oxide based gas sensors. *J. Appl. Phys.* **1994**, *76* (8), 4467−4471.

(15) Wang, Y.; Djerdj, I.; Smarsly, B.; Antonietti, M. Antimony-Doped SnO_2 Nanopowders with High Crystallinity for Lithium-Ion Battery Electrode. *Chem. Mater.* **2009**, *21* (14), 3202−3209.

(16) Hong, S.-N.; Kye, Y.-H.; Yu, C.-J.; Jong, U.-G.; Ri, G.-C.; Choe, C.-S.; Kim, K.-H.; Han, J.-M. Ab initio thermodynamic study of the SnO_2 (110) surface in an O_2 and NO environment: a fundamental understanding of the gas sensing mechanism for NO and NO_2. *Phys. Chem. Chem. Phys.* **2016**, *18* (46), 31566−31578.

(17) Liang, L. Y.; Liu, Z. M.; Cao, H. T.; Pan, X. Q. Microstructural, Optical, and Electrical Properties of SnO Thin Films Prepared on Quartz via a Two-Step Method. *ACS Appl. Mater. Interfaces* **2010**, *2* (4), 1060−1065.

(18) Tamura, H.; Mita, K.; Tanaka, A.; Ito, M. Mechanism of Hydroxylation of Metal Oxide Surfaces. *J. Colloid Interface Sci.* **2001**, *243* (1), 202−207.

(19) Li, Y.; Meng, L.; Yang, Y.; Xu, G.; Hong, Z.; Chen, Q.; You, J.; Li, G.; Yang, Y.; Li, Y. High-efficiency robust perovskite solar cells on ultrathin flexible substrates. *Nat. Commun.* **2016**, *7* (1), 10214.

(20) Yang, D.; Yang, R.; Wang, K.; Wu, C.; Zhu, X.; Feng, J.; Ren, X.; Fang, G.; Priya, S.; Liu, S. High efficiency planar-type perovskite solar cells with negligible hysteresis using EDTA-complexed SnO_2. *Nat. Commun.* **2018**, *9* (1), 3239.

(21) Ching-Prado, E.; Samudio, C. A.; Santiago-Aviles, J.; Velumani, S. Electronic structure and optical properties of SnO_2:F from PBE0 hybrid functional calculations. *J. Mater. Sci.: Mater. Electron.* **2018**, *29* (18), 15423−15435.

(22) Anaraki, E. H.; Kermanpur, A.; Steier, L.; Domanski, K.; Matsui, T.; Tress, W.; Saliba, M.; Abate, A.; Grätzel, M.; Hagfeldt, A.; Correa-Baena, J.-P. Highly efficient and stable planar perovskite solar cells by solution-processed tin oxide. *Energy Environ. Sci.* **2016**, *9* (10), 3128−3134.

(23) Luo, D.; Su, R.; Zhang, W.; Gong, Q.; Zhu, R. Minimizing non-radiative recombination losses in perovskite solar cells. *Nat. Rev. Mater.* **2020**, *5* (1), 44−60.

https://dx.doi.org/10.1021/acsenergylett.0c01566
ACS Energy Lett. 2020, 5, 2796−2801